

Article

Conditions for Minimizing the Computational Complexity of the RCWA Calculation of the Diffraction Efficiency of Sawtooth Two-Layer Double-Relief Microstructures

Grigoriy I. Greisukh ^{1,*} , Artem I. Antonov ¹, Evgeniy G. Ezhov ¹, Viktor A. Danilov ² and Boris A. Usievich ³

¹ Physics Department, Penza State University of Architecture and Construction, G. Titova Str., 440028 Penza, Russia; gromlord@yandex.ru (A.I.A.); phisik@pguas.ru (E.G.E.)

² Scientific and Technological Center for Unique Instrumentation, Russian Academy of Sciences, Butlerova Str., 117342 Moscow, Russia; viktordanilov@bk.ru

³ Prokhorov General Physics Institute, Russian Academy of Sciences, Vavilov Str., 119991 Moscow, Russia; borisu@kapella.gpi.ru

* Correspondence: grey@pguas.ru

Abstract: In this study, novel recommendations are presented and substantiated for selecting the number of modes and optical thicknesses of flat lattice slabs that make up microreliefs, which minimize the computational complexity of the rigorous coupled-wave analysis calculation of the diffraction efficiency (DE) of a sawtooth two-layer two-relief microstructure, while maintaining the specified reliability of the calculation results. The computational complexity can be controlled by allowing one or another level of oscillation of the DE curves, depending on the angle of incidence of the radiation incident on the microstructure. In particular, the complexity of the thousands of DE calculations in the optimization process can be reduced by using the proposed methodology as well as increased computational complexity to verify the accuracy of the solution obtained as a result of the implemented optimization.

Keywords: two-layer two-relief diffractive microstructure; diffraction efficiency; scalar and rigorous theories of diffraction; rigorous coupled-wave analysis



Citation: Greisukh, G.I.; Antonov, A.I.; Ezhov, E.G.; Danilov, V.A.; Usievich, B.A. Conditions for Minimizing the Computational Complexity of the RCWA Calculation of the Diffraction Efficiency of Sawtooth Two-Layer Double-Relief Microstructures. *Photonics* **2023**, *10*, 794. <https://doi.org/10.3390/photonics10070794>

Received: 11 May 2023

Revised: 27 June 2023

Accepted: 7 July 2023

Published: 10 July 2023



Copyright: © 2023 by the authors. Licensee MDPI, Basel, Switzerland. This article is an open access article distributed under the terms and conditions of the Creative Commons Attribution (CC BY) license (<https://creativecommons.org/licenses/by/4.0/>).

1. Introduction

Diffractive optical elements (DOEs) with annular microstructures similar to that of a Fresnel zone plate have attracted the attention of developers of imaging optical systems because of their unique aberration properties. In the field of chromaticism, DOEs are characterized by a negative dispersion. Moreover, in the field of monochromatic aberrations, DOEs are characterized by the automatic fulfillment of the Petzval condition and a rapid convergence of the aberration expansion for planar DOEs [1,2]. Properties of DOEs included in an optical system consisting of refractive lenses provide tangible advantages.

However, the last statement is valid only if the ratio of the radiation flux diffracted into the working order to that incident on the microstructure, i.e., the diffraction efficiency (DE) of the DOE microstructure, neither falls below a given level in the entire working spectral range nor over the entire range of angles of incidence of the radiation incident on this microstructure.

The maximum DE among the existing technologies for manufacturing ring quasi-periodic microstructures is provided by relief-phase microstructures. A single-layer microstructure (Figure 1a) can have $DE = 1$, but only at one specific wavelength and for one specific angle of incidence of radiation, i.e., this microstructure has energy selectivity with regard to wavelength spectrum and angle of incidence. Two-layer, one- or two-relief microstructures have been successfully used to suppress spectral energy selectivity, as shown in Figure 1b–d [3–7].

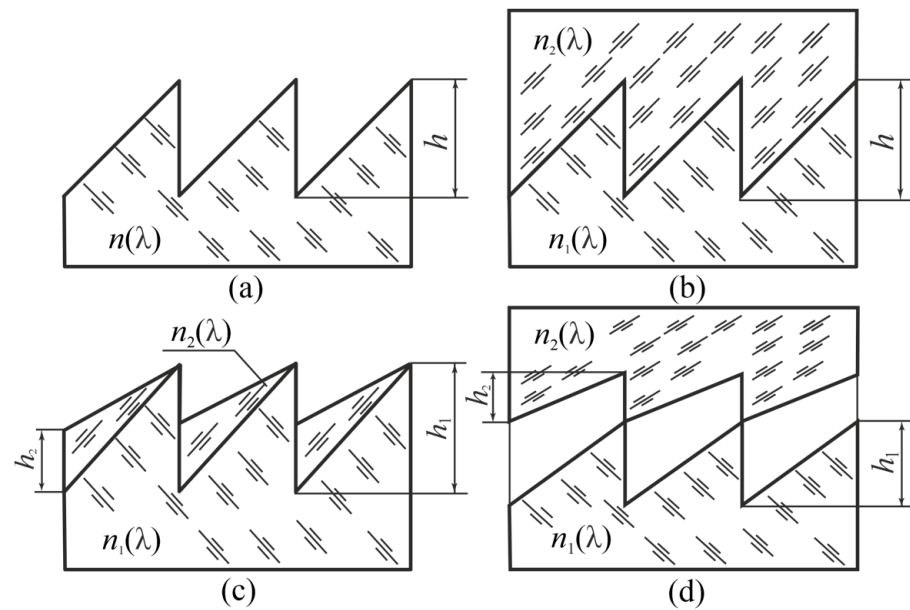


Figure 1. DOE relief-phase microstructures: (a) a single-layer microstructure; (b) a two-layer one-relief microstructure; (c,d) two-layer two-relief microstructures.

The energy angular selectivity is more pronounced for two-layer microstructures than for single-layer microstructures; moreover, its minimization is ensured by minimizing the effective depths of the reliefs h_{eff} ($h_{\text{eff}} = h, h_1,$ and $h_1 + h_2$ in the schemes in Figure 1b, Figure 1c, and Figure 1d, respectively). Assuming that the spectral energy selectivity is suppressed, the effective depths of the reliefs are minimized using an appropriate choice of pairs of optical materials in the microstructure arrangement.

Furthermore, the catalog of optical materials from which a pair of materials can be selected for a two-layer, single-relief microstructure, as shown in Figure 1b, is significantly narrow, even in the visible range. This is because a material with a high refractive index should also have a higher Abbe number, a well-known requirement for pairs of materials with two-layer, single-relief microstructures [4,6]. If a certain number of such pairs, including heavy crown and light flint, are available from optical glasses, they are then completely absent from technological and commercially available optical plastics.

This limitation is eliminated due to the two reliefs made in the two optical materials with different dispersion properties. In addition, despite the obvious appeal (in terms of angular-energy selectivity) of a microstructure with one internal relief (Figure 1c), in some cases, the choice may favor the microstructure shown in Figure 1d. This primarily applies to infrared (IR) optics that operate over a wide range of temperatures. Indeed, owing to the different thermal coefficients of linear expansion of the two layers of the microstructure, as shown in Figure 1c, ensuring mechanical strength at significantly different operating temperatures is impossible. Therefore, the most acceptable arrangement of the IR DOE microstructure currently is a two-layer microstructure with two internal sawtooth reliefs on the flat surfaces of the material substrates.

The search for optimal pairs of optical materials for the DOE microstructure is based on determining the optimal relief depths for each pair of optical materials; this requires multiple calculations of DE. As reported in [8], the results obtained based on the DEs calculated using the scalar effective area method (EAM) [9,10] are fairly reliable in the layout and calculation of microstructures intended for operation in the IR and visible range [9,10]. This applies to a greater extent to selecting the optimal pairs of optical materials, but to a lesser extent to assessing the optimal depths of the reliefs and to assessing the achievable DE.

Indeed, the degree of reliability in determining the optimal depths and achievable DE depends on the given interval of angles of incidence of radiation incident on the

microstructure for the selected relative (normalized to the total depth of the reliefs) spatial period of the microstructure $P = \Lambda / (h_1 + h_2)$. Finally, these scalar results may be unreliable for microstructures with a total relief depth greater than the maximum wavelength of the working spectral range by an order of magnitude. The truly optimal relief depths of such microstructures, as well as microstructures designed for wide ranges of radiation incidence angles ($\pm 15^\circ$ and more), and a reliable estimate of their DEs can only be obtained by optimizing in the framework of rigorous diffraction theory and solving the system of Maxwell equations. In this case, a good initial approximation is obtained using the scalar EAM method.

Currently, the most common numerical methods for solving systems of Maxwell equations to calculate DE are the rigorous coupled-wave analysis (RCWA) [11,12] and finite-difference time-domain (FDTD) methods [9]. The insurmountable disadvantage of the latter method is that it requires considerably more computational time and computer RAM. Therefore, the RCWA method is preferred for calculating the DE of sawtooth microstructures. In particular, this method involves replacing the sawtooth relief of the diffractive microstructure with a set of flat lattice plates and applying a Fourier expansion to the periodically distributed permittivity of each plate. The accuracy of this method is determined by the optical thickness of the flat lattice slabs L that make up both microreliefs and the number of modes N_m . The computational complexity of the RCWA method depends on the aforementioned parameters.

The results of the RCWA analysis of the microstructures presented in this study are obtained using two software platforms developed with the participation of the authors of this paper, namely, PSUAC-DE [13] and MC Grating Software [14]. The PSUAC-DE algorithm is based on the enhanced transmittance matrix approach [15] while the MC Grating Software algorithm does not differ from that proposed by Maharam [11,12].

Considering that in general, the DOEs of imaging optical systems operate with unpolarized radiation, DE calculation should include calculating the efficiencies for transverse electric (TE) and transverse magnetic (TM) polarized waves; moreover, the arithmetic mean of the obtained values is considered the resulting DE. However, in the practical calculation of the DEs of all types of microstructures as shown in Figure 1, the computational complexity in the case of a TM wave is much greater, whereas the resulting efficiency values for TE and TM waves differ by no more than 2–3%, as confirmed in this study. Therefore, in this study, the efficiency calculated for the TE wave is considered as the DE obtained using the RCWA method.

However, even in this case, the duration of the computational process for calculating the DE of deep relief-phase structures (two-layer microstructures with two internal reliefs) may not be acceptable for optimizing the design parameters of the microstructure. To this end, this study proposes novel recommendations for selecting the values of the main computational parameters L and N_m to ensure the minimum computational time with guaranteed reliability of the calculation results.

2. Visible Spectral Range

One of the most pronounced signs of the inadequacy of the values of the computational parameters L and N_m in the target problem is the oscillation of the DE curves, showcasing the dependence of DE on the incidence angle of the radiation incident on the microstructure. Evidently, oscillations prevent not only the determination of the optimal depths of the reliefs, but also a reliable assessment of the maximum permissible angle of incidence.

To clarify the causes of the oscillations and exclude the effect of Fresnel losses on the DE, antireflection coatings on the working surfaces of the microstructure are modeled into the calculation, as shown in Figure 2.

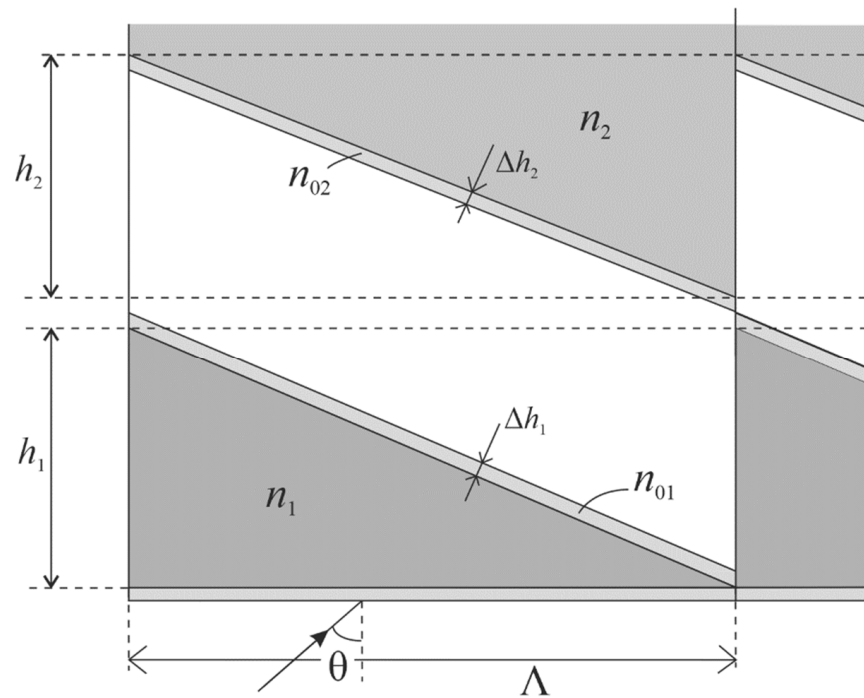


Figure 2. Two-layer, two-relief microstructure with coatings deposited on the reliefs.

The space between the reliefs in the microstructure materials with refractive indices n_1 and n_2 is filled with air; moreover, the sharp peaks of the reliefs are in contact with coatings with thicknesses of Δh_1 and Δh_2 and refractive indices of n_{01} and n_{02} , respectively. The model coverage parameters for each wavelength are calculated using the following formulas:

$$n_{0i} = \sqrt{n_i}; \Delta h_i = 0.25\lambda/n_{0i} \tag{1}$$

where $i = 1, 2$.

The calculations are performed for a microstructure [7] with a lower layer of E48R crown-like optical plastic ($n_d = 1.531160$; $\nu_d = 56.0438$) included in the ZEON catalog of the ZEMAX optical design software [16] and an upper layer of EP7000 flint-like optical plastic ($n_d = 1.651006$; $\nu_d = 21.4946$) manufactured by MITSUBISHI GAS CHEMICAL under the trademark, Lupizeta™ EP7000 [17]. The calculations are performed in the visible spectral range from $\lambda_{\min} = 0.4 \mu\text{m}$ to $\lambda_{\max} = 0.7 \mu\text{m}$.

In the calculations, the radiation is assumed to be incident on the microstructure from the air onto the side of the medium with refractive index n_1 , the angle of incidence θ is measured from the normal to the substrate, and the diffracted radiation remains in the medium with refractive index n_2 . This is because the output of the diffracted radiation through a flat surface with a model antireflection coating would only increase DE calculation complexity without affecting the its results.

Figures 3 and 4 illustrate the dependence of DE on the angle of incidence obtained at two values of the relative spatial period of the microstructure $P = 10$ and $P = 30$. The number of plates in each of the two reliefs and number of modes $N_p = N_m = 200$ ensured the absence of oscillations at $P = 30$ and the fulfillment of the following condition:

$$\sum_i (DE_{ti} + DE_{ri}) = 1 \tag{2}$$

Here, DE_{ti} and DE_{ri} are the diffraction efficiencies in transmitted and reflected orders, respectively. During the calculations, we considered all diffraction orders with numbers $(1 - N_m/2) \leq i \leq N_m/2$.

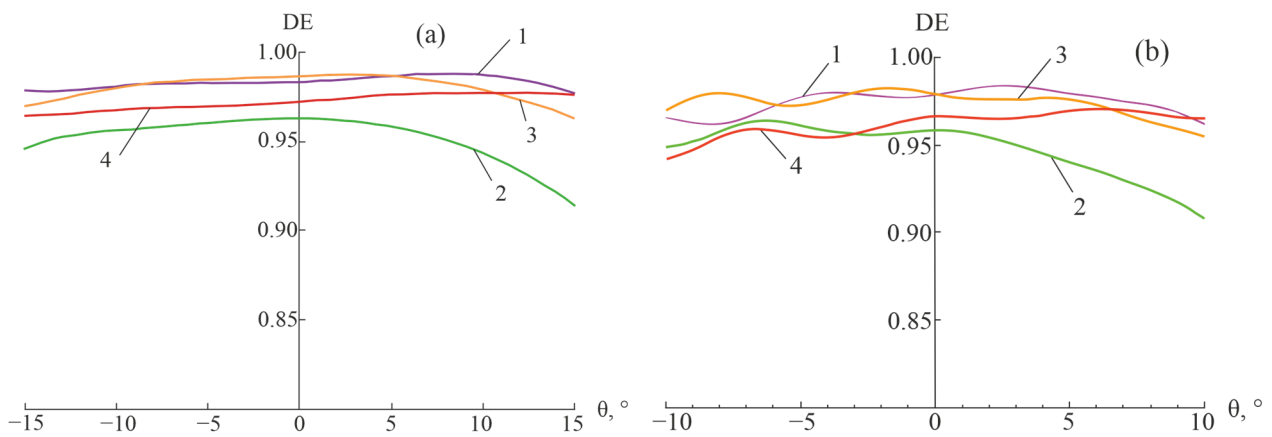


Figure 3. Dependencies of the DE of E48R/EP7000 microstructure on the angle of incidence for multiple wavelengths: (a) $h_1 = 8.792 \mu\text{m}$, $h_2 = 6.268 \mu\text{m}$, and $P = 30$; and (b) $h_1 = 8.792 \mu\text{m}$, $h_2 = 6.246 \mu\text{m}$, and $P = 10$; curved lines 1, 2, 3 and 4 at $\lambda = 0.4, 0.5, 0.6$ and $0.7 \mu\text{m}$, respectively.

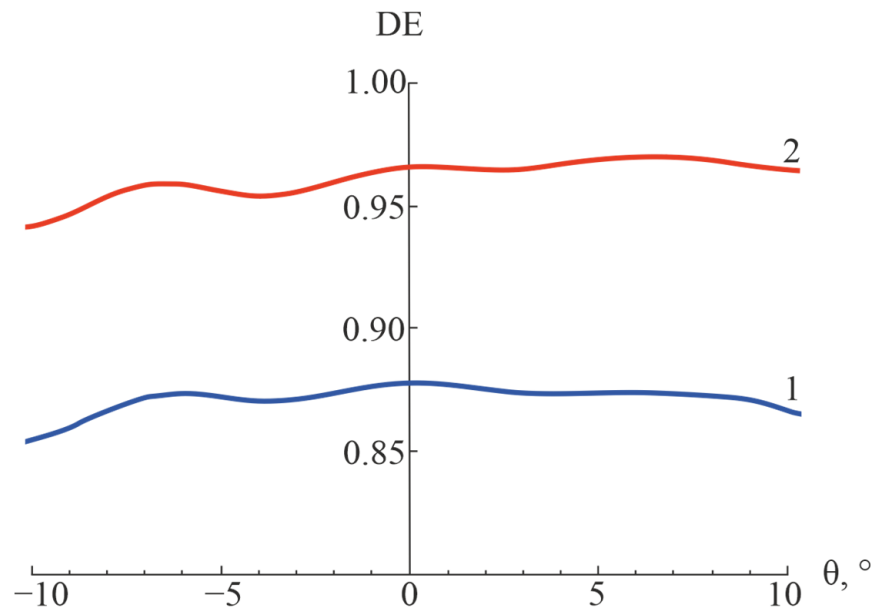


Figure 4. Dependencies of the DE of E48R/EP7000 microstructure on the angle of incidence for $\lambda = 0.7 \mu\text{m}$ and $P = 10$ (curved line 1 is the case of without modeling of antireflection coatings; curved line 2 is the case of with modeling of antireflection coatings).

Considering that the oscillations are most pronounced at $P = 10$ and $\lambda = 0.7 \mu\text{m}$, the calculation is performed with these parameters for the case without antireflection coatings (Figure 4).

The calculation results presented in Figures 3 and 4 confirm that the oscillating nature of the dependence of DE on the angle of incidence is not associated with the Fresnel reflection of radiation from flat or relief working surfaces of the microstructure; moreover, these dependences are identically retained even after almost completely suppressing the reflections. In particular, the oscillation amplitudes do not depend on the presence or absence of antireflection coatings, and the maximum oscillation amplitudes of curves 1, A_{n1} , and 2, A_{n2} , normalized by the constant component of DE are 0.72% and 0.65%, respectively.

A novel, in-depth analysis of the influence of the parameters L and N_m on the level of DE and oscillations is presented next. Moreover, E48R/EP7000 microstructure with the model antireflection coatings is used for analysis. In this case, the optical thicknesses

of the plates in both layers are assumed equal, i.e., $L = n_1 \cdot l_{h1} = n_2 \cdot l_{h2} = k\lambda$. The analysis demonstrates that the optical thicknesses of the plates in the range of $0.08 \leq k \leq 0.32$ have almost no effect on the oscillations, but significantly affect the DE level. Furthermore, the number of modes ($50 \leq N_m \leq 600$) affects both the DE level and oscillations. These trends are clearly confirmed by the graphs in Figure 5 obtained at the central wavelength of the visible spectral range $\lambda = 0.55 \mu\text{m}$ at $h_1 = 8.792 \mu\text{m}$, $h_2 = 6.246 \mu\text{m}$, and $P = 10$. At $N_m = 50$, the curves corresponding to all values of k merge, and the DE level is the lowest (Figure 5a). At $N_m = 200$, the oscillations are pronounced (normalized oscillation amplitude $A_n = 0.53\%$ at $k = 0.32$), and the DE level increases with decreasing k (Figure 5b). At $N_m = 400$, the oscillations decrease to an acceptable level, and the DE level, similar to that in Figure 5b, increases with decreasing k (Figure 5c). A further decrease in k leads to merging of the curves with a slight increase in the DE level and $A_n \leq 0.07\%$ at $k = 0.12$ (Figure 5d). Here, for all TE-polarization calculations, regardless of the values of k and N_m , condition (2) is satisfied. Therefore, a decrease in the DE in the first (working) diffraction order automatically leads to an increase in the DE in the side orders.

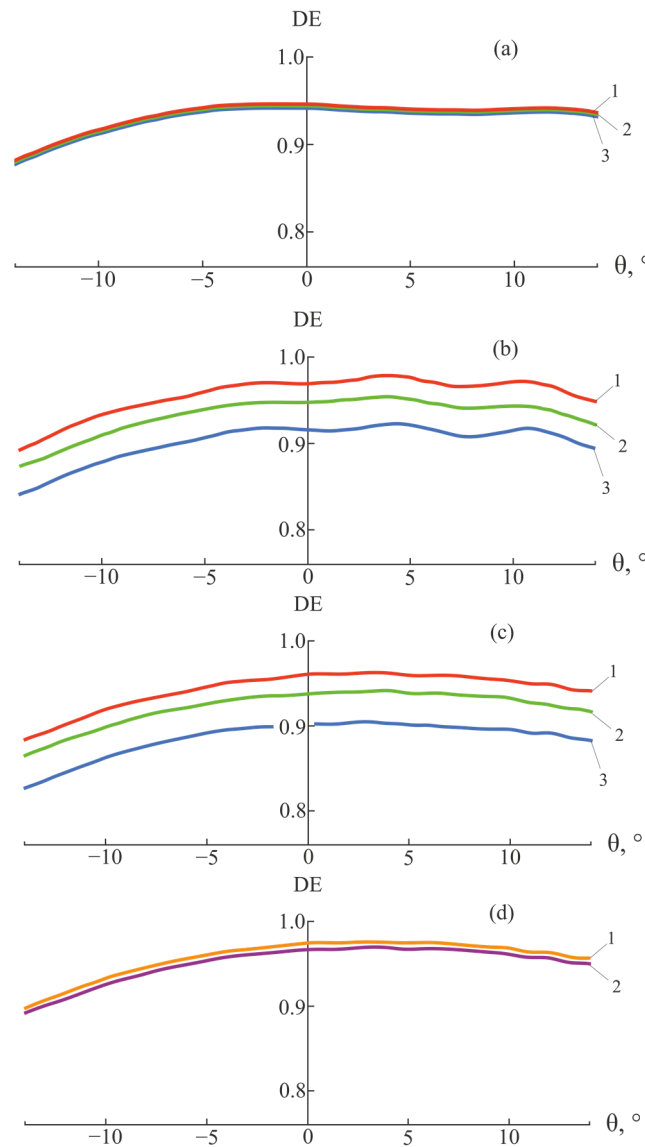


Figure 5. Dependences of the DE of E48R/EP7000 microstructure on the angle of incidence at a wavelength of $\lambda = 0.55 \mu\text{m}$ at $P = 10$: (a) $N_m = 50$; (b) $N_m = 200$; and (c) $N_m = 400$; curved lines 1, 2, and 3 at $k = 0.16, 0.24$, and 0.32 , respectively. (d) $N_m = 400$; curved lines 1 and 2 at $k = 0.08$ and 0.12 , respectively.

The calculation time increases with decreasing k and increases depending on N_m , usually according to a quadratic law. Accordingly, the maximum value of k and the minimum value of N_m can be used at which oscillations do not significantly affect the calculation results. In the case under consideration, $k \leq 0.12$ and $N_m = 300$ at $\lambda = 0.55 \mu\text{m}$ (Figure 6a). Furthermore, at other wavelengths of the working spectral range, the oscillations can have a slightly larger amplitude, requiring a decrease in k to 0.08 and an increase in N_m to 400 for their almost complete suppression (Figure 6b).

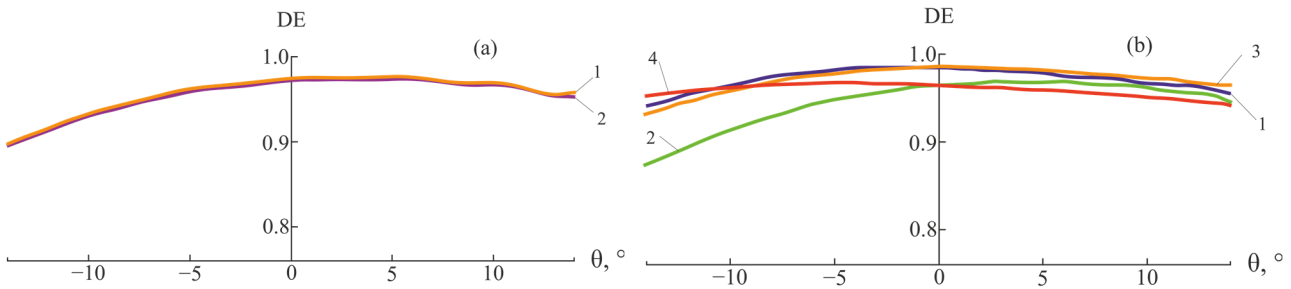


Figure 6. Dependences of the DE of E48R/EP7000 microstructure on the angle of incidence at $P = 10$: (a) $N_m = 300$ at a wavelength of $\lambda = 0.55 \mu\text{m}$ (curved lines 1 and 2 at $k = 0.08$ and 0.12 , respectively) and (b) $N_m = 400$ and $k = 0.08$ at four visible wavelengths (curved lines 1, 2, 3 and 4 at $\lambda = 0.4, 0.5, 0.6$ and $0.7 \mu\text{m}$, respectively).

A double increase in the relative spatial period of the microstructure ($P = 20$) does not affect the recommended value of the k parameter ($k \leq 0.12$), but requires an increase in the recommended value of the N_m parameter ($N_m \geq 500$, see Figure 7). Indeed, at $N_m = 400$ and $600 A_n \leq 0.068\%$, and $N_m \leq 0.043\%$ (in both cases $k = 0.16$).

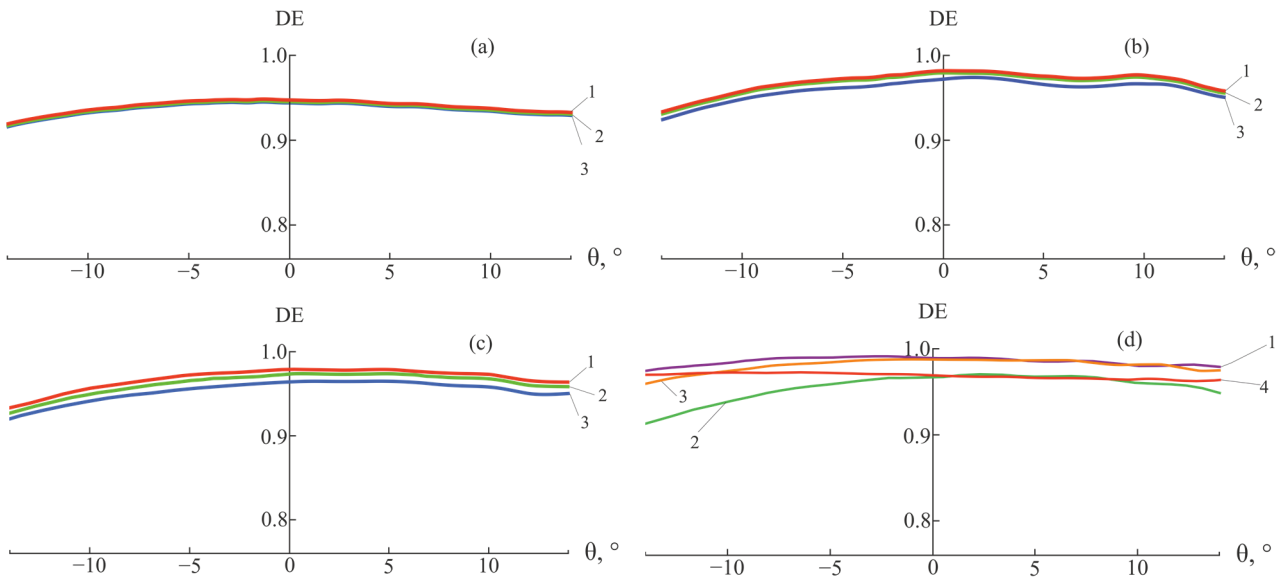


Figure 7. Dependences of the DE of E48R/EP7000 microstructure on the angle of incidence at $P = 20$: (a) $N_m = 50$ and $\lambda = 0.55 \mu\text{m}$; (b) $N_m = 400$ and $\lambda = 0.55 \mu\text{m}$; and (c) $N_m = 600$ and $\lambda = 0.55 \mu\text{m}$ (curved lines 1, 2, and 3 at $k = 0.08, 0.12$ and 0.16 , respectively). (d) $N_m = 600$ and $k = 0.08$ at four visible wavelengths (curved lines 1, 2, 3, and 4 at $\lambda = 0.4, 0.5, 0.6,$ and $0.7 \mu\text{m}$, respectively).

Comparing the recommended N_m values obtained for this microstructure at $P = 10$ and $P = 20$, the following simple relation is valid:

$$N_m > P(h_1 + h_2)/\lambda, \tag{3}$$

where λ is the central wavelength of the working spectral range.

Note that, as pointed out in [7,18], an increase in the spatial period of the microstructure allows expanding the range of radiation incidence angles within which the DE does not fall below a given level.

Similar calculations for two-layer microstructures with two internal sawtooth reliefs composed of pairs of optical plastics, namely, PMMA/POLYCARB, E48R/POLYSTYR, and E48R/ITO in PMMA [7] result in the same recommended k and N_m values. Moreover, this does not depend on whether PSUAC-DE or MC Grating Software is used for calculations.

Furthermore, we present one of the typical results of calculating DE for two cases: TM and TE polarization. This calculation was performed for the E48R/EP7000 microstructure at $P = 10$ and $k = 0.32$ at a wavelength $\lambda = 0.55 \mu\text{m}$ over three angles of incidence of radiation $\theta = 0^\circ$ and $\theta = \pm 14^\circ$. The increase in computational complexity for TM polarization is associated not so much with an increase in the required number of N_m modes taken into account, as with the need to select the N_m value to fulfill condition (2) (see Table 1).

Table 1. Diffraction efficiency of the E48R/EP7000 microstructure at two types of polarization.

Angle of Incidence, °	TM Polarization						TE Polarization at $N_m = 200$
	N_m	DE	N_m	DE	N_m	DE	
−14	200	0.825	314	0.837	406	0.863	0.841
0		0.914	300	0.917	420	0.905	0.915
14		0.619	302	0.888	416	0.886	0.893

The data in Table 1 show that with optimal selection of the number of modes for each angle of incidence of radiation, the difference in the DE values calculated for the TM and TE polarizations does not exceed 2.6%. However, this results in a significant increase in computational complexity.

3. Infrared Spectral Range

In this section, we investigate how the optical thickness of the plates L and the number of modes N_m influence the relationship between the DE of microstructures and the angle of incidence of IR radiation. These microstructures belong to the DOEs of several refractive-diffractive objectives designed by the authors of this article. The objectives were designed to operate in the dual IR range, including medium-wavelength IR (MWIR) (3.4–5.2 μm) and long-wavelength IR (LWIR) (7.5–11.4 μm) subranges.

The results of the study are demonstrated by the example of two microstructures, SRF2/GERMANIUM ($h_1 = 53.6 \mu\text{m}$ and $h_2 = 8.71 \mu\text{m}$) and PBF2/GASIR1 ($h_1 = 87.36 \mu\text{m}$ and $h_2 = 44.12 \mu\text{m}$). Three materials of their layers (SRF2, PBF2, and GERMANIUM) are obtained from the INFRARED catalog of the ZEMAX program; moreover, GASIR1 is obtained from the UMICORE catalog [19]. The choice of these microstructures is not accidental. They both have a fairly high DE at $|\theta| \leq 14^\circ$, whereas the refractive indices of the respective layers differ by more than 1.2 and 1.6 times (Table 2).

Table 2. Refractive indices of IR optical materials at the central wavelengths of the MWIR and LWIR sub-bands.

$\lambda, \mu\text{m}$	n_1			n_2
	SRF2	PBF2	GERMANIUM	GASIR1
4.3	1.410538	1.714346	4.021764	2.509057
9.45	1.319191	1.646837	4.004906	2.496018

In the calculations, as in the visible range, the radiation is assumed to be incident on the microstructure from the air onto the side of the medium with the refractive index n_1 ,

the angle of incidence θ is measured from the normal to the substrate, and the diffracted radiation remains in the medium with the refractive index n_2 . In this case, the optical thicknesses of the plates in both layers are assumed equal, i.e., $L = n_1 \cdot l_{h1} = n_2 \cdot l_{h2} = k\lambda$.

Figure 8 shows the dependence curves of the DE for the SRF2/GERMANIUM microstructure with regard to the angle of incidence, obtained using PSUAC-DE program at $P = 10$.

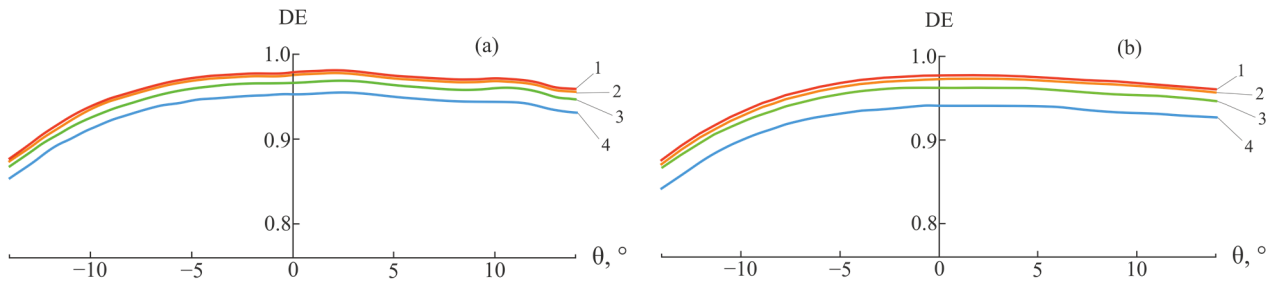


Figure 8. Dependences of the DE of SRF2/GERMANIUM microstructure on the angle of incidence for a wavelength of $\lambda = 4.3 \mu\text{m}$ and $P = 10$: (a) $N_m = 200$ and (b) $N_m = 400$ (curved lines 1, 2, 3 and 4 at $k = 0.05, 0.075, 0.1$ and 0.15 , respectively).

At $N_m = 200$, the oscillations are insignificant ($\Delta n \leq 0.06\%$ at $k = 0.1$), whereas at $N_m = 400$, they disappear completely. In this case, a k value of less than 0.05 does not make sense. This is true for all dual-IR wavelengths (Figure 9).

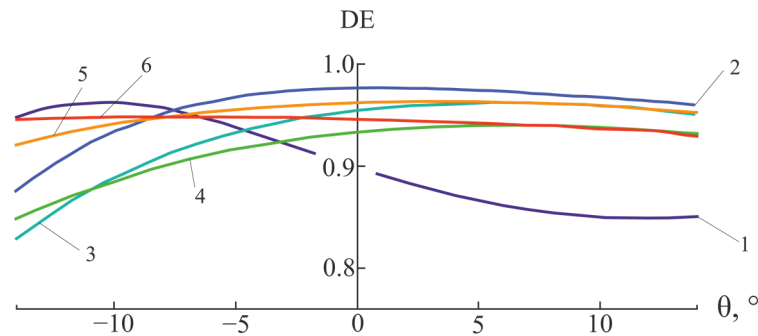


Figure 9. SRF2/GERMANIUM DE versus angle of incidence at $P = 10$, $N_m = 400$, and $k = 0.05$ for six dual-IR wavelengths: curved lines 1, 2, 3, 4, 5, and 6 at $\lambda = 3.4, 4.3, 5.2, 7.5, 9.45$, and $11.4 \mu\text{m}$, respectively.

A two-fold increase in the relative spatial period of the microstructure in this case does not affect the recommended value of the parameter k , but requires an increase in the number of modes to reduce the oscillation amplitude to an acceptable level (Figures 10 and 11).

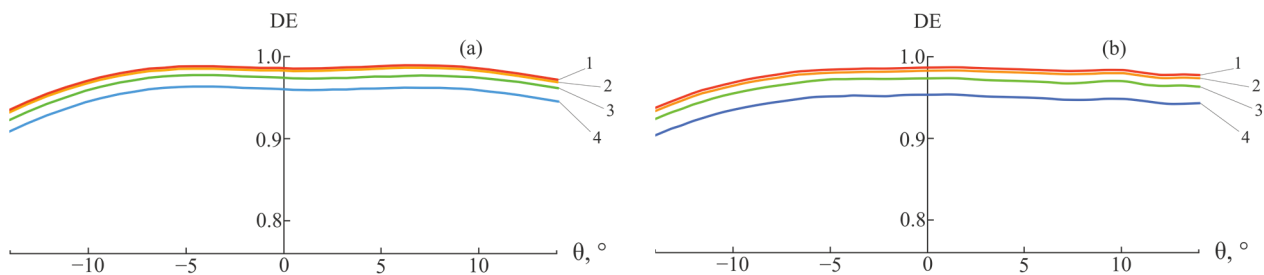


Figure 10. Dependences of the DE of SRF2/GERMANIUM microstructure on the angle of incidence for a wavelength of $\lambda = 4.3 \mu\text{m}$ and $P = 20$: (a) $N_m = 200$ and (b) $N_m = 400$ (curved lines 1, 2, 3, and 4 at $k = 0.05, 0.075, 0.1$, and 0.15 , respectively).

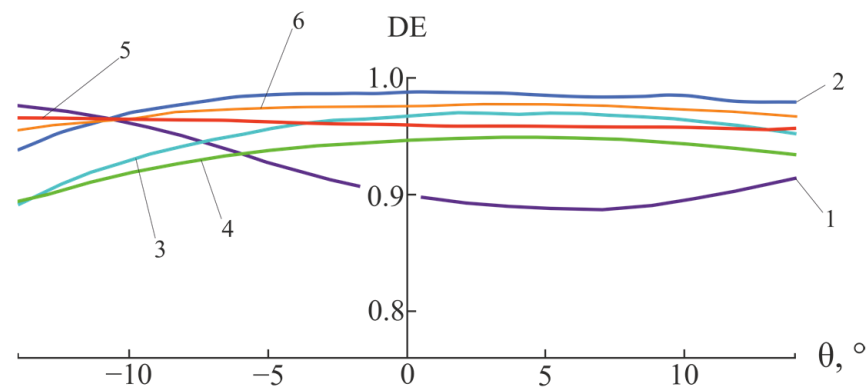


Figure 11. SRF2/GERMANIUM DE versus angle of incidence at $P = 20$, $N_m = 400$, and $k = 0.05$ for six dual-IR wavelengths: curved lines 1, 2, 3, 4, 5, and 6 at $\lambda = 3.4, 4.3, 5.2, 7.5, 9.45,$ and $11.4 \mu\text{m}$, respectively.

By comparing the k values used in the visible and IR ranges as well as the refractive indices of E48R/EP7000 and SRF2/GERMANIUM microstructures, the following empirical formula is proposed for the relationship between the corresponding k values:

$$k_{IR} \approx k_{Vis} n_2^{(Vis)} / n_2^{(IR)}, \tag{4}$$

where k_{IR} and k_{Vis} are the k parameters of the second layer of the microstructure at the central wavelengths of the MWIR and visible ranges, respectively. Similarly, $n_2^{(IR)}$ are $n_2^{(Vis)}$ are the corresponding refractive indices.

An analysis of the influence of the k and N_m parameters on the level and oscillations of the DE of PBF2/GASIR1 microstructure is conducted at the values of k calculated using Equation (4). The results for $P = 10$ case are presented in Figure 12.

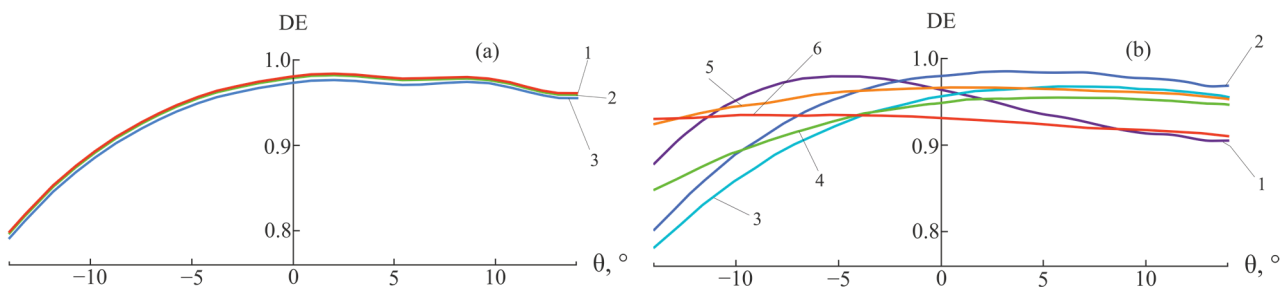


Figure 12. Dependences of the DE of PBF2/GASIR1 microstructure on the angle of incidence at $P = 10$: (a) $N_m = 200$ for a wavelength of $\lambda = 4.3 \mu\text{m}$ (curved lines 1, 2, and 3 at $k = 0.105, 0.158$ and 0.21 , respectively) and (b) $N_m = 400$ and $k = 0.105$ for six wavelengths of dual IR (curved lines 1, 2, 3, 4, 5 and 6 at $\lambda = 3.4, 4.3, 5.2, 7.5, 9.45$ and $11.4 \mu\text{m}$, respectively). At $\lambda = 4.3 \mu\text{m}$ ($k = 0.105$) $A_n \leq 0.036\%$ at $N_m = 200$ and $A_n \leq 0.022\%$ at $N_m = 400$.

An increase in the relative spatial period of the microstructure to $P = 20$ does not affect the recommended value of the parameter k in the case of this microstructure; however, a two-fold increase in the number of modes is required, which reduces the oscillation amplitude to an acceptable level.

Note that in the IR and visible ranges, an increase in the spatial period of the microstructure allows expanding the range of radiation incidence angles within which the DE does not fall below a given level.

Summarizing the results presented in Sections 2 and 3, the value obtained via Equation (3) should be considered as the recommended number of modes for all microstructures in both the visible and IR ranges. As for the parameter k , based on Formula (4), it should be taken

as its recommended value $k \leq 0.264/n_2$, where n_2 is the larger of the two refractive indices of the microstructure layers at the central wavelength of the visible or MWIR ranges.

Obviously, an increase in the relative spatial period, which allows the expansion of the range of angles of incidence of radiation incident on the microstructure, inevitably increases the computational complexity of the RCWA calculation of the DE.

4. Discussion

The unique aberration properties of the DOE, when is included in the optical scheme of the refractive lens system, results in a significant positive effect both in the visible and IR ranges. However, the latter is true only if the DE of the DOE microstructure neither falls below a specific level in the entire working spectral range nor over the entire range of the angles of incidence of the radiation incident on this microstructure. A two-layer microstructure with two internal sawtooth reliefs [7,20] fully satisfies these requirements over a wide range of operating temperatures [18].

In several previous studies, the results of using a rigorous diffraction theory based on the solution of Maxwell equations for calculating the DE of multilayer sawtooth microstructures have been presented [6–9,11,12,20–26].

However, in these studies devoted to the use of the FDTD and RCWA methods for calculating the DE of single-layer binary and sawtooth microstructures, as well as for calculating the DE of two-layer one- or two-relief sawtooth microstructures, the problem of minimizing the computational complexity of these methods has not been considered. At best, individual recommendations aimed at reducing computational process time have been cited without evidence. Furthermore, the computational complexity of electromagnetic methods often exceeds that of scalar methods. This problem stimulated the search for a new effective method for arranging and calculating two-relief microstructures within the framework of the scalar theory of diffraction, considering the real depths of sawtooth reliefs. To this end, EAM has been proposed [9,10]. The advantage of EAM is that it allows truly selecting the optimal pairs of optical materials for sawtooth two-layer two-relief microstructures intended for operation in both the visible and IR ranges [8]. However, a reliable estimate of the optimal relief depths and DE levels of such microstructures within the given ranges of radiation incidence angles in multiple cases can only be obtained through optimization within the framework of a rigorous diffraction theory. The practical possibility of such an optimization is primarily determined by the computational complexity of the DE calculations.

In relation to the RCWA method, this paper presents several simple empirical formulas for estimating the number of modes and flat lattice plates, which are sufficient to obtain reliable DE calculation results. This eliminates the loss of time due to unnecessary calculations with inflated parameters.

5. Conclusions

The DOE of imaging optical systems in both the visible and IR ranges must have a high DE within the working spectral range and within a given range of angles of incidence of radiation incident on the microstructure. These requirements are satisfied, in particular, by the elements with a sawtooth two-layer two-relief microstructure. In this case, a reliable and optimal pair of optical materials for such a microstructure can be selected within the framework of the scalar theory of diffraction. However, truly optimal relief depths and a reliable assessment of the DE level of the microstructure within a given range of radiation incidence angles can be obtained, in most cases, only as a result of electromagnetic optimization, particularly using the RCWA method. The accuracy of this method is determined by the optical thicknesses of the flat lattice slabs $L = n_1 \cdot l_{h1} = n_2 \cdot l_{h2} = k\lambda$ that make up both the microreliefs and the number of modes N_m , i.e., the harmonics of the Fourier series. The computational complexity of the calculations also depends on these parameters.

The recommendations proposed and substantiated in this study on selecting the number of modes and optical thickness of the plates (Equations (3) and (4)) allow the

minimization of the computational complexity of the RCWA calculation of the DE of a sawtooth two-layer two-relief microstructure while maintaining the specified reliability of the calculation results.

Moreover, the computational complexity can be controlled through the relationship $N_m = C\Lambda/\lambda$, i.e., by allowing one or another level of oscillation of the DE curves, depending on the angle of incidence. By setting $C \leq 1$, the complexity of multiple DE calculations can be reduced in the optimization process. Moreover, by setting $C > 1$, the computational complexity can be increased to certify the accuracy of the solution obtained as a result of implemented optimization.

Author Contributions: Conceptualization, methodology, writing—original draft preparation, G.I.G. and E.G.E.; validation, software, formal analysis, A.I.A., V.A.D. and B.A.U.; visualization, A.I.A. All authors have read and agreed to the published version of the manuscript.

Funding: This research was funded by the Russian Science Foundation (Project No. 20-19-00081).

Institutional Review Board Statement: Not applicable.

Informed Consent Statement: Informed consent was obtained from all subjects involved in the study.

Data Availability Statement: Not applicable.

Conflicts of Interest: The authors declare no conflict of interest.

References

1. Greisukh, G.I.; Bobrov, S.T.; Stepanov, S.A. *Optics of Diffractive and Gradient-Index Elements and Systems*; SPIE Press: Bellingham, WA, USA, 1997; 414p.
2. Wood, A.; Babington, J. *Diffractive Lens Design: Theory, Design, Methodologies and Applications (Emerging Technologies in Optics and Photonics)*; Iop Publishing Ltd.: Bristol, UK, 2023; 300p.
3. Arieli, Y.; Ozeri, S.; Eisenberg, N. Design of a diffractive optical element for wide spectral bandwidth. *Opt. Lett.* **1998**, *23*, 823–824. [[CrossRef](#)] [[PubMed](#)]
4. Lukin, A.V. Holographic optical elements. *J. Opt. Technol.* **2007**, *74*, 65–70. [[CrossRef](#)]
5. Zhao, Y.H.; Fan, C.J.; Ying, C.F.; Liu, S.H. The investigation of triple-layer diffraction optical element with wide field of view and high diffraction efficiency. *Opt. Commun.* **2013**, *295*, 104–107. [[CrossRef](#)]
6. Greisukh, G.I.; Yezhov, Y.G.; Antonov, A.I.; Danilov, V.A.; Usievich, B.A. Potential opportunities of sawtooth diffraction microstructure with two layers and single relief. *J. Opt.* **2020**, *22*, 085604. [[CrossRef](#)]
7. Greisukh, G.I.; Danilov, V.A.; Ezhov, E.G.; Kazin, S.V.; Usievich, B.A. Highly Efficient Double-Layer Diffraction Microstructures Based on New Plastics and Molded Glasses. *Photonics* **2021**, *8*, 327. [[CrossRef](#)]
8. Greisukh, G.I.; Ezhov, E.G.; Antonov, A.I.; Danilov, V.A.; Usievich, B.A. Comparative analysis estimates for two-relief microstructures diffraction efficiency in the visible and dual infrared ranges in the framework of scalar and rigorous diffraction theories. *J. Opt. Technol.* **2023**, *in print*.
9. Yang, H.; Xue, C.; Li, C.; Wang, J.; Zhang, R. Diffraction efficiency sensitivity to oblique incident angle for multilayer diffractive optical elements. *Appl. Opt.* **2016**, *55*, 7126–7133. [[CrossRef](#)] [[PubMed](#)]
10. Yang, C.; Yang, H.; Li, C.; Xue, C. Optimization and analysis of infrared multilayer diffractive optical elements with finite feature sizes. *Appl. Opt.* **2019**, *58*, 2589–2595. [[CrossRef](#)] [[PubMed](#)]
11. Moharam, M.G.; Grann, E.B.; Pommet, D.A.; Gaylord, T.K. Formulation for stable and efficient implementation of the rigorous coupled-wave analysis of binary gratings. *JOSA* **1995**, *12*, 1068–1076. [[CrossRef](#)]
12. Moharam, M.G.; Pommet, D.A.; Grann, E.B.; Gaylord, T.K. Stable implementation of the rigorous coupled-wave analysis for surface-relief gratings: Enhanced transmittance matrix approach. *JOSA* **1995**, *12*, 1077–1086. [[CrossRef](#)]
13. Antonov, A.I.; Greisukh, G.I.; Kazin, S.V. PSUAC-DE. Russian Federation Certificate of State Registration of the Computer Program. Russian Patent No. 2022681578, 15 November 2022.
14. Lyndin, N.M. Modal and C Methods Grating Design. Available online: <http://www.mcgrating.com> (accessed on 12 April 2023).
15. Antonov, A.I.; Greisukh, G.I. Approach for finding amplitudes of the transmitted diffraction orders in the framework of a rigorous coupled-wave analysis and its application in the study of three-layer sawtooth microstructures. In Proceedings of the Holography, Diffractive Optics, and Applications X, Online, 11–16 October 2020; Volume 115511C. [[CrossRef](#)]
16. Zemax Source. Available online: <http://www.zemax.com/pages/opticstudio> (accessed on 12 April 2023).
17. Mitsubishi Gas Chemical. Available online: http://www.mgc.co.jp/eng/products/kc/iupizeta_ep.html (accessed on 12 April 2023).
18. Greisukh, G.I.; Levin, I.A.; Ezhov, E.G. Design of Ultra-High-Aperture Dual-Range Athermal Infrared Objectives. *Photonics* **2022**, *9*, 742. [[CrossRef](#)]

19. UMICORE Electro-Optic Materials Source. Available online: <https://eom.umicore.com/en/infrared-solutions/infrared-optics/introducing-gasir> (accessed on 12 April 2023).
20. Greisukh, G.I.; Ezhov, E.G.; Zakharov, O.A.; Danilov, V.A.; Usievich, B.A. Limiting spectral and angular characteristics of sawtooth dual-relief two-layer diffraction microstructures. *Quantum Electron.* **2021**, *51*, 184–188. [[CrossRef](#)]
21. Hakko, M.; Kiire, T.; Barada, D.; Yatagai, T.; Hayasaki, Y. Shape estimation of diffractive optical elements using high-dynamic range scatterometry. *Appl. Opt.* **2015**, *54*, 4255–4261. [[CrossRef](#)]
22. Di, F.; Yingbai, Y.; Guofan, J.; Qiaofeng, T.; Liu, H. Rigorous electromagnetic design of finite-aperture diffractive optical elements by use of an iterative optimization algorithm. *JOSA A* **2003**, *20*, 1739–1746. [[CrossRef](#)] [[PubMed](#)]
23. Lee, Y.J.; Kim, Y.H.; Park, C.M.; Yang, J.K. Analysis of optical propagation characteristics of the ultra-long period grating using RCWA. *Appl. Opt.* **2023**, *62*, 2376–2385. [[CrossRef](#)] [[PubMed](#)]
24. Zhang, B.; Cui, Q.; Piao, M. Effect of substrate material selection on polychromatic integral diffraction efficiency for multilayer diffractive optics in oblique incident situation. *Opt. Commun.* **2018**, *415*, 156–163. [[CrossRef](#)]
25. Francés, J.; Bleda, S.; Gallego, S.; Neipp, C.; Márquez, A.; Pascual, I.; Beléndez, A. Accuracy analysis of simplified and rigorous numerical method applied to binary nanopatterning gratings in non-paraxial domain. *Phys. Lett. A* **2013**, *377*, 2245–2250. [[CrossRef](#)]
26. Xu, Q.; Chen, X.; Li, C.; Guo, Y.; Chen, X.; Xu, Y. Design of 2-layer transmission grating with high efficiency, large bandwidth and great dispersion. In Proceedings of the Holography, Diffractive Optics, and Applications X, Online, 11–16 October 2020; Volume 115511D. [[CrossRef](#)]

Disclaimer/Publisher’s Note: The statements, opinions and data contained in all publications are solely those of the individual author(s) and contributor(s) and not of MDPI and/or the editor(s). MDPI and/or the editor(s) disclaim responsibility for any injury to people or property resulting from any ideas, methods, instructions or products referred to in the content.